



Dynamics of mercury stable isotope compounds in Arctic seals: New insights from a controlled feeding trial on hooded seals *Cystophora cristata*[☆]

Marianna Pinzone^{a,*}, David Amouroux^b, Emmanuel Tessier^b, Mario Acquarone^c, Ursula Siebert^d, Krishna Das^{a,**}

^a Freshwater and Oceanic Sciences Unit of ReSearch (FOCUS), Laboratory of Oceanology, University of Liège, Liège, Belgium

^b Université de Pau et des Pays de L'Adour, E2S UPPA, CNRS, IPREM, Institut des Sciences Analytiques et de Physico-chimie pour L'Environnement et Les Matériaux, Pau, France

^c Arctic Monitoring and Assessment Programme, The Fram Centre, Tromsø, Norway

^d Institute for Terrestrial and Aquatic Wildlife Research (ITAW), University of Veterinary Medicine Hannover, Foundation, Bismarck, Germany

ARTICLE INFO

Keywords:

Hg stable isotopes
Arctic seals
Bioaccumulation
Demethylation
Tissue metabolism

ABSTRACT

Accurate interpretation of mercury (Hg) isotopic data requires the consideration of several biotic factors such as age, diet, geographical range, and tissue metabolic turnover. A priori knowledge of prey-predator isotopic incorporation rates and Hg biomagnification is essential. This study aims to assess Hg stable isotopes incorporation in an Arctic species of Phocidae, the hooded seal *Cystophora cristata*, kept in human care for 24 months (2012–2014) and fed on a constant diet of Norwegian Spring Spawning herring *Clupea harengus*. We measured THg, MMHg and iHg levels, as well as Hg stable isotope composition with both mass dependent (MDF) and mass independent (MIF) fractionation (e.g. $\delta^{202}\text{Hg}$ and $\Delta^{199,200,201,204}\text{Hg}$) in hooded seal kidney, liver, hair and muscle, in addition to herring muscle. We then calculated Hg MDF and MIF isotopic fractionation between hooded seals and their prey. We found a significant shift in $\delta^{202}\text{Hg}$ between hooded seal hair (+0.80‰) and kidney (−0.78‰), and herring muscle. In hooded seals tissues $\delta^{202}\text{Hg}$ correlated positively with MMHg percentage. These findings suggest that tissue-specific Hg speciation is the major driver of changes in Hg isotopic fractionation rates in this Arctic predator. $\Delta^{199}\text{Hg}$, $\Delta^{200}\text{Hg}$, $\Delta^{201}\text{Hg}$ and $\Delta^{204}\text{Hg}$ values did not vary between herring and hooded seal tissues, confirming their utility as tracers of Hg marine and atmospheric sources in top predators. To our knowledge, this represents the first attempt to assess complex Hg isotope dynamics in the internal system of Arctic Phocidae, controlling the effects of age, diet, and distribution. Our results confirm the validity of Hg stable isotopes as tracers of environmental Hg sources even in top predators, but emphasize the importance of animal age and tissue selection for inter-study and inter-species comparisons.

1. Introduction

The assessment of mercury (Hg) sources and pathways in the marine environment remains a complex challenge despite its recognized toxicity for both wildlife and humans. Monomethyl-Hg (MMHg) is considered the most toxic form of Hg to marine predators, as it bioaccumulates within food webs and biomagnifies from one trophic level to another (Lehnherr, 2014). The toxic effects of MMHg to marine predators are governed by *in vivo* processes such as transformation, intratissue exchange, and detoxification rates and pathways (Poulin

et al., 2021). In marine mammals, MMHg transformations mostly include MMHg demethylation in liver, while the main elimination pathways are molting and excretion (Wagemann et al., 1998).

The analysis of Hg stable isotope composition is increasingly carried out in marine organisms to study Hg sources and trophic transfer (Kwon et al., 2020). Over the last 20 years, the number of publications on the application of *in vivo* Hg stable isotopes analysis has quadrupled (Meng et al., 2020). Because mass independent isotopic fractionation (MIF; e.g., $\Delta^{199}\text{Hg}$, $\Delta^{201}\text{Hg}$ for odd isotopes) is not influenced by organisms' metabolism and does not change from one trophic level to the other, it

[☆] This paper has been recommended for acceptance by Dr Michael Bank.

* Corresponding author.

** Corresponding author.

E-mail addresses: mpinzone@uliege.be (M. Pinzone), krishna.das@uliege.be (K. Das).

can be successfully used to trace MMHg or inorganic Hg(II) (iHg) sources from the environment to marine predators (Cransveld et al., 2017; Kwon et al., 2014; Le Croizier et al., 2020). Hg mass dependent fractionation (MDF, measured by $\delta^{202}\text{Hg}$) reflects the Hg isotope values of MMHg in the ambient environment and can be used to study Hg biogeochemical cycling in the marine ecosystem (Tsui et al., 2019). However, since Hg MDF is caused by numerous processes, the range of $\delta^{202}\text{Hg}$ values found in aquatic ecosystems is very wide (-3 to 2‰), making their interpretation quite complex (Zhou et al., 2023). $\delta^{202}\text{Hg}$ values can efficiently help interpret Hg dynamics within the organisms. In seabirds, marine mammals and fish a significant Hg MDF can occur between different tissue of an organism during Hg uptake and metabolism (transfer, transformation and excretion) (Feng et al., 2015; Man et al., 2019; Pinzone et al., 2022; Wang and Tan, 2019). Additionally, a significant prey-predator Hg MDF was found to occur in the higher trophic levels of food webs (Tsui et al., 2019; Perrot et al., 2010). Both tissue-specific and trophic isotope fractionations were found to vary between species and ecosystems (Tsui et al., 2019). While the processes of internal Hg isotope fractionation have been fully described in birds, only about ten studies have focuses on marine mammals, living several questions about Hg metabolic processing still open (Li et al., 2022). Accurate interpretation of isotopic fractionation requires consideration of several biotic factors such as sex, age, diet, habitat use and geographical distribution (Pinzone et al., 2017). Its quantification at a species-specific level is essential to correctly assess potential differences in the rates of Hg trophic transfer between marine predators with different life cycles, physiologies, and trophic ecology.

Arctic true seals present important physiological and ecological adaptations to survive in a cold and extreme environment (Blix, 2005). Such adaptations might strongly influence Hg isotope fractionation within the organism. The hooded seal *Cystophora cristata* is an Arctic true seal, which relies on drifting ice during breeding and moulting season (Øigå et al., 2014). The hooded seal is one of the most contaminated Arctic true seals, presenting hepatic Hg concentrations (e.g., Julshamn & Grahl-Nielsen (Julshamn and Grahl-Nielsen, 2000), 2000: $1368\text{--}239400\text{ ng g}^{-1}\text{ dw}$; or Pinzone M. (Pinzone et al., 2021a), PhD 2021: $158\text{--}320618\text{ ng g}^{-1}\text{ dw}$) often surpassing the toxicity thresholds proposed for humans and wildlife (Julshamn and Grahl-Nielsen, 2000; Brunborg et al., 2006; Nielsen and Dietz, 1990; Sonne et al., 2009). Hooded seals exhibit intense physiological and feeding adaptations that enhance the chances of survival of newborns in the harsh Arctic environment (Blix, 2016). For example, the hooded seal's lactation period, lasting only 4 days, is the shortest ever recorded for mammals and is characterised by extreme mother-pup energy transfer as well as body mass shifts (Bowen et al., 1985; Hoff et al., 2017). Such adaptations might exacerbate Hg remobilization within the organism, potentially contributing to the heavier accumulation of Hg in their body compared to other seal species (Routti et al., 2018). This makes the hooded seal one of the species most at risk of adverse health effects related to Hg contamination (Dietz et al., 2013). Understanding the dynamics of Hg in hooded seals is imperative for thorough health risk assessments at population scale (Dietz et al., 2019; Eagles-Smith et al., 2018) and provides insights into contaminant dynamics in other Arctic mammals.

The calculation of isotope fractionation has successfully allowed quantitative assessment of the rate and extent of MDF of elements like carbon (C), nitrogen (N) and sulfur (S) between prey and consumers (Pinzone et al., 2017; Germain et al., 2013; Caut et al., 2009). Previously we proposed that the intense metabolic changes hooded seal pups undergo during growth enhance prey-consumer C, N and S isotope fractionation compared to other seals species (Pinzone et al., 2017). This question remains open in the case of Hg isotope fractionation by both *in vivo* and trophic processes. Previous studies on marine mammals like polar bears, seals and pilot whales (Bolea-Fernandez et al., 2019; Li et al., 2020; Perrot et al., 2015) were conducted on wild animals. As such the effects of environmental processes on Hg MDF and MIF remained a confounding factor in the interpretation of Hg metabolism by the

organisms.

In this study we aimed to (1) assess Hg trophic isotope fractionation between hooded seals and their prey, and (2) identify the main mechanisms of *in vivo* isotope fractionation between the different tissues of an Arctic top predator. To achieve these two objectives, we determined Hg stable isotopes composition in several tissues of hooded seals in human care, kept on a constant diet composed of herrings *Clupea harengus*. We compared our findings with existing literature on marine predators such as marine mammals or seabirds, to identify additional factors (e.g., age) that may influence Hg isotopic fractionation in our seals. The paper presents the first attempt to conduct a long-term controlled experiment to characterize tissue-specific Hg isotope fractionation without the interference of diet, age, or distribution, reflecting only the basal metabolization of Hg within a specialized Arctic marine predator. Our results have important implications for the growing interest in using Hg isotopes for biomonitoring, which requires precise characterization of internal Hg isotope fractionation in various biota.

2. Materials and methods

2.1. Sampling and controlled experiment

Samples from several tissues of eight hooded seals in human care used in this work derive from the tissue specimen bank of previous studies at the University of Tromsø (Norway) and the University of Liege (Belgium). The animals were primarily used for experiments other than those reported here. Details of both the ethical protocol and the controlled experiment are published elsewhere (Pinzone et al., 2017; Geiseler et al., 2016; Alvira-Iraizoz et al., 2019). Briefly, eight post-weaned hooded seal newborns were captured in March 2012, on the whelping grounds along the pack-ice of the Greenland Sea, North-West of Jan Mayen Island (Li et al., 2022) (Table S1). Sampling was conducted during a research cruise with R/V *Helmer Hanssen*. Seals were captured with the use of a hoop-net and transited back to Tromsø (Norway). The holding facility was situated at the Department of Arctic and Marine Biology (DAMB), UiT – the Arctic University of Tromsø (UiT). For 24 months, all seals were fed on a constant diet of same-size Norwegian Spring Spawning herring *Clupea harengus* (Pelagia – Seafood from Norway, MSC-C-50933, FAO 27; 2 kg/animal per day (Gentry and Holt, 1982)), supplemented with a vitamin complex (Seatabs MA III, Pacific Research Labs, Inc., Vashon Island, WA, USA). The herring originated from the same area of the Norwegian Sea and were fished at the same time of the year, always during spring season, which minimised biases from seasonal isotopic variability. The seals were euthanized in accordance with a permit issued by the National Animal Research Authority of Norway (NARA permit no. 5399, 5422 and 5843): the seals were sedated by intramuscular injection of zolazepam/tiletamine (Zoletil Forte Vet., Virbac S.A., France; $1.5\text{--}2.0\text{ mg kg}^{-1}$ body mass), then anaesthetized using an endotracheal tube to ventilate lungs with 2–3 % isoflurane (Forene, Abbott, Germany) in air before administering an intravenous overdose of pentobarbital (Euthasol vet. Le Vet B.V. Netherlands; $\sim 30\text{ mg per kg}$ of body mass). Muscle of hooded seals and herring (entire fish, $n = 30$) and liver, kidney, and hair of hooded seals were collected after dissection with ceramic utensils and stored in -20 °C freezers at the Department of Arctic Marine Biology at UiT.

2.2. Samples preparation

Between 6 and 10 g of thawed tissue (muscle, liver, kidney and hair) were dissected using a ceramic knife (or scissors), placed in plastic tubes, and accurately weighted to the nearest 0.1 mg. Tubes were then placed at -80 °C overnight before freeze-drying for 48 h (Alpha 1–4 LD plus, Christ, Germany). Hair samples were washed ultrasonically with reagent grade acetone (acetone for trace analysis $\geq 99.8\%$ purity, ARISTAR®, VWR) and were rinsed repeatedly with Milli-Q water ($18.2\text{ M}\Omega\text{ cm}^{-1}$) to remove exogenous contaminants, blood, and fat residuals, according to

the method recommended by the International Atomic Energy Agency (Katz and Chatt, 1988). Hair samples were lyophilized for 24h. Muscle, liver and kidney samples were ground to a fine powder using a ceramic mortar and pestle, while hairs were cut with ceramic scissors to the smallest size possible.

2.3. Total-mercury analysis

Total Hg concentrations (hereafter expressed as ng g^{-1} dry weight, dw) were quantified by atomic absorption spectroscopy (AAS) on a Tri-cell Direct Mercury Analyzer 80 (DMA-80 Evo, Milestone, Italy), in compliance with the US EPA 7473 protocol validated for biological solid samples and solutions. Between 5 and 30 mg of sample material were loaded in quartz boats and weighted to the nearest 0.01 mg. Quality assurance for the analysis included using blanks (HCL 1 %), standard solutions ($100 \text{ ng Hg mL}^{-1}$, Merck) and certified reference materials (CRMs) at the beginning and end of each batch: DOLT-4 ($n = 5$), ERM-CE464 ($n = 6$), NIES-13 ($n = 8$, Table S3). THg recovery ranged from 86 to 93% for DOLT-4, from 94 to 96% for ERM-CE464 and from 97 to 104% for NIES-13.

2.4. Mercury species analysis

Samples preparation and Hg species analysis followed the same protocol previously developed for Arctic seals tissues and published elsewhere (Table S2) (Masbou et al., 2015). Hair Hg extraction was conducted through acid digestion using nitric acid HNO_3 -6N (INSTRA-ANALYZED J.T.Baker) solution prepared in ultrapure H_2O (Milli-Q, Millipore). Hg extraction in muscle, liver and kidney was conducted through an alkaline digestion by tetramethylammonium hydroxide TMAH 25 % ($(\text{CH}_3)_4\text{NOH}$ in H_2O , Sigma Aldrich). Between 50 and 150 mg of samples were digested in 5 mL of reagent. Solutions were left to rest overnight in digestion vials (CEM) at room temperature. Microwave assisted extraction was performed using a CEM MW system Discover SP-D, coupled to an Explorer autosampler (CEM Corporation, USA) at a controlled temperature of 75°C . Prior to Hg species analyses, samples were derivatized at pH 4 by ethylating, using sodium tetraethyl borate (NaBEt_4 , 5 %, Merseburger Spezialkemikalien). Hg species concentrations were quantified by species-specific isotopic dilution mass spectrometry analysis (SIDMS) as previously described (Renedo et al., 2017). Quantification was conducted with the single-IDA method, based on the measurement of the mixed isotope ratios (Clé et al., 2012; Rodríguez-González et al., 2005). Spiking was conducted before digestion for hair tissue (acid digestion), while for muscle, liver and kidney it was done afterwards (basic digestion). Hg species analysis was carried out by GC-ICPMS Trace Ultra GC equipped with a Triplus RSH autosampler coupled to an ICP-MS Xseries II (Thermo Scientific, USA). The quality assurance protocol included the analysis of 3 replicates for each sample, the use of blanks and CRMs with the same proportion of MMHg and iHg as our samples (Table S2): ERM-CE464 (tuna fish muscle, ERM®), DOLT-4 (dogfish liver, CNRC), and NIES-13 (Human hair, NIES). The robustness of the two independent analytical methodologies employed (DMA 80 and GC-ICPMS) was validated by comparing the measured THg contents with the sum of the iHg and MMHg contents exhibiting an average recovery of $99 \pm 7\%$ for the samples set ($n = 40$). Recovery % of all Hg species are reported for each CRM in Table S2.

2.5. Mercury stable isotopes analysis

Samples preparation and Hg stable isotopes analysis followed the same method previously published elsewhere (Renedo et al., 2018). Between 50 and 150 mg of hair, muscle, kidney and liver were digested in blue-cap 50 mL falcon vials adding 3 mL of HNO_3 (69 %, INSTRA-ANALYZED J.T.Baker) and 1 mL of HCL (37 %, INSTRA-ANALYZED J.T.Baker). Samples were left to digest at room temperature, overnight. A first round of digestion was then achieved at

85°C during 24 h, using a heating HotBlock device (HB). After cooling, 1 mL of H_2O_2 (30 %, ULTREX II J.T.Baker) was added to the vessels before operating a second HB digestion for other 24 h. Hg isotopic analyses were then performed in a Nu Plasma MC-ICPMS (Nu Instruments, UK using a continuous flow Cold Vapor Generation (CVG)). Internal reproducibility of the analytical method was performed on the medium and long-term through repetition of the measurement of CRMs (DOLT-5, ERM-CE464 and NIES-13), the NIST RM-8610 (UM-Almaden) and selected seal samples (Table S4). Our measurements fell within the uncertainty range of previous studies conducted in other laboratories with other extraction and analytical techniques (Li et al., 2020; Li et al., 2014; Epov et al., 2008; Sherman et al., 2013; Yamakawa et al., 2016) as well as studies conducted at the same laboratory between 2008 and 2022 (Perrot et al., 2010; Masbou et al., 2013; Bé et al., 2017; Pinzone et al., 2021b; Queipo-Abad et al., 2022; Renedo et al., 2021) (Table S3). The long-term precision (2SD) for Hg isotopic values was satisfactory for the most analyzed reference samples: RM-8610 (0.07 ‰ and 0.06 ‰, $n = 12$), DOLT-5 (0.14 ‰ and 0.16 ‰, $n = 7$), ERM-CE464 (0.14‰ and 0.21‰, $n = 4$) and NIES-13 (0.12 ‰ and 0.17 ‰, $n = 3$) for $\delta^{202}\text{Hg}$ and $\Delta^{199}\text{Hg}$ values, respectively.

Hg isotopic values were reported as delta (δ) notation values (in permil, ‰), calculated relative to the bracketing standard NIST SRM-3133 CRM (approximate uncertainty of $\pm 15\%$) to allow interlaboratory comparisons (Supporting Information, Section 1.2). NIST SRM-997 thallium standard solution was used for the instrumental mass-bias correction using the exponential law. The δ sign represents mass dependent fractionation (MDF) and was calculated as follows:

$$\delta^{202}\text{Hg} = \left\{ \left[\frac{\left(\frac{\text{H}_{202}\text{g}}{\text{H}_{198}\text{g}} \right)_{\text{sample}}}{\left(\frac{\text{H}_{202}\text{g}}{\text{H}_{198}\text{g}} \right)_{\text{NIST} - 3133}} \right] - 1 \right\} \times 1000$$

Δ represents mass independent fractionation (MIF) and was calculated as follows:

$$\Delta^{199}\text{Hg} \approx \delta^{199}\text{Hg} - (\delta^{202}\text{Hg} \times 0.2520)$$

$$\Delta^{200}\text{Hg} \approx \delta^{200}\text{Hg} - (\delta^{202}\text{Hg} \times 0.5024)$$

$$\Delta^{201}\text{Hg} \approx \delta^{201}\text{Hg} - (\delta^{202}\text{Hg} \times 0.7520)$$

$$\Delta^{204}\text{Hg} \approx \delta^{204}\text{Hg} - (\delta^{202}\text{Hg} \times 1.4930)$$

2.6. Statistical analyses

Data normality was tested with the Shapiro-Wilk test, recommended for small sample size. The skewness, kurtosis, and Mean-Median difference were calculated to select which statistical tests to use (parametric vs. non-parametric). Kurtosis and skewness are typically used to describe the data tail's spread and the symmetry of the distribution, respectively. When data are normal, skewness equals 0 and kurtosis equals 3. Although most data followed a Gaussian distribution, the kurtosis was < 3 and skewness > 1 for most of data groups, indicating an asymmetrical tendency of the curve. For many groups, the mean did not equal the median. Due to these reasons and the small sample size (e.g., $n = 4$ for hair), non-parametric tests were used.

Pairwise comparisons were done with the Mann-Whitney test. Otherwise, the Kruskal-Wallis (KW) test followed by Dunnett's multiple comparison was performed. The Spearman rho (ρ) was used to assess correlation between parameters. All statistical analysis was conducted in R (version 4.0.5; R Core Team, 2018). Family-wise significance and confidence level was set at $\alpha = 0.05$ (95 % confidence interval). However, due to the small n of certain groups and the large Hg isotopic variability, differences with p value > 0.01 were not interpreted.

Table 1
 THg, MMHg and iHg concentrations (in ng g⁻¹ dw), fMMHg and iHg fractions (fMMHg and fiHg, in %) and Hg stable isotope composition (as “delta” notation in ‰) measured in hooded seal *C. cristata* pups in human care and their prey, the herring *C. harengus*. Results are shown as Mean (Median) ± SD (Min – Max). *n* equals the number of organisms on which the analysis was conducted. Statistical groups resulting from the Kruskal-Wallis non-parametric analysis are reported in superscript, italic letters (*a* to *d*). The alpha was set to 0.01.

Animal	Hooded Seal			Herring		
	Tissue	Liver	Muscle	Hair	Muscle	Muscle
<i>n</i>	6	6	6	4	18	18
THg ng g ⁻¹ dw	7875 ^{6a} (7349) ± 3521 (2674–12624)	5376 ^{6a} (4676) ± 2659 (2427–9152)	540 ^b (574) ± 110 (348–640)	1171 ^{b,c} (1194) ± 346 (622–1592)	108 ^b (86.7) ± 52.0 (47.8–191)	108 ^b (86.7) ± 52.0 (47.8–191)
MMHg ng g ⁻¹ dw	814 ^{6a} (881) ± 150 (562–1014)	537 ^b (529) ± 110 (354–707)	453 ^b (474) ± 113 (270–588)	1070 ^c (1104) ± 318 (531–1484)	100 ^d (73.8) ± 50.7 (46.1–186)	100 ^d (73.8) ± 50.7 (46.1–186)
iHg ng g ⁻¹ dw	6686 ^{6a} (7019) ± 3099 (1967–10026)	4454 ^{6a} (4122) ± 1973 (1750–7363)	990 ^b (102) ± 27.5 (50.8–140)	114 ^d (116) ± 24 (74–147)	9.37 ^b (6.36) ± 5.72 (2.01–24.3)	9.37 ^b (6.36) ± 5.72 (2.01–24.3)
fMMHg %	16.9 ^{6a} (13.8) ± 8.59 (7.18–25.8)	16.4 ^{6a} (15.5) ± 8.34 (5.67–24.8)	81.5 ^b (81.2) ± 5.28 (73.5–92.5)	89.8 ^{6a} (90.1) ± 2.86 (85.7–93.2)	88.4 ^{b,c} (91.5) ± 9.45 (55.6–94.9)	88.4 ^{b,c} (91.5) ± 9.45 (55.6–94.9)
fiHg %	85.7 ^a (90.3) ± 9.54 (67.3–91.5)	87.1 ^a (88.5) ± 7.08 (74.3–95.1)	18.5 ^b (20.1) ± 5.51 (9.75–24.6)	10.1 ^{b,c} (9.9) ± 2.83 (6.66–14.3)	1.35 ^a (7.94) ± 2.92 (3.71–16.6)	1.35 ^a (7.94) ± 2.92 (3.71–16.6)
δ ²⁰² Hg ‰	0.71 ^{6a} (0.63) ± 0.36 (0.50–0.97)	0.22 ^{6a} (0.17) ± 0.26 (0.09–0.47)	1.20 ^{6a} (1.27) ± 0.76 (0.75–1.74)	1.79 ^{6a} (1.72) ± 0.45 (1.62–2.11)	1.00 ^{6a} (0.92) ± 0.38 (0.79–1.46)	1.00 ^{6a} (0.92) ± 0.38 (0.79–1.46)
Δ ¹⁹⁹ Hg ‰	1.16 ^{6a} (1.13) ± 0.13 (1.08–1.23)	1.08 ^{6a} (1.08) ± 0.02 (1.06–1.09)	1.16 ^{6a} (1.14) ± 0.12 (1.12–1.30)	1.12 ^{6a} (1.13) ± 0.05 (1.10–1.15)	0.97 ^{6a} (0.91) ± 0.35 (0.60–1.25)	0.97 ^{6a} (0.91) ± 0.35 (0.60–1.25)
Δ ²⁰⁰ Hg ‰	0.02 ⁶ (0.02) ± 0.06 (–0.03–0.07)	–0.01 ⁶ (–0.01) ± 0.03 (–0.03–0.02)	0.06 ⁶ (0.05) ± 0.10 (0.01–0.17)	0.02 ⁶ (0.02) ± 0.04 (0.00–0.04)	0.03 ⁶ (0.03) ± 0.07 (–0.05–0.09)	0.03 ⁶ (0.03) ± 0.07 (–0.05–0.09)
Δ ²⁰¹ Hg ‰	0.99 ⁶ (1.00) ± 0.09 (0.91–1.03)	0.93 ⁶ (0.92) ± 0.04 (0.90–0.96)	1.00 ⁶ (0.98) ± 0.16 (0.93–1.19)	0.99 ⁶ (0.98) ± 0.05 (0.96–1.01)	0.81 ⁶ (0.75) ± 0.32 (0.59–1.07)	0.81 ⁶ (0.75) ± 0.32 (0.59–1.07)
Δ ²⁰⁴ Hg ‰	–0.04 ⁶ (–0.03) ± 0.15 (–0.16–0.05)	–0.03 ⁶ (–0.01) ± 0.11 (–0.11–0.04)	–0.01 ⁶ (–0.02) ± 0.16 (–0.10–0.16)	–0.08 ⁶ (–0.07) ± 0.06 (–0.11 to –0.04)	–0.05 ⁶ (–0.04) ± 0.16 (–0.24–0.06)	–0.05 ⁶ (–0.04) ± 0.16 (–0.24–0.06)

* Data variability within analytical uncertainty and/or the statistical differences considered as weak since *p* values ranged between >0.01 and 0.05.

3. Results

3.1. Total-mercury

THg concentrations in hooded seals followed the trend: liver ≈ kidney > hair ≈ muscle (Table 1), with significant differences between tissues (KW = 34.3, *p* < 0.0001). THg concentrations in the liver and kidney of hooded seals were significantly higher than in herring (Dunnett: *p* < 0.0001 and *p* < 0.0001, respectively). THg concentrations did not differ significantly between hooded seal muscle and hair and herring muscle (Table 1).

3.2. Mercury species

MMHg concentrations in hooded seals followed the trend: hair > liver > kidney ≈ muscle (Table 1), with significant differences between tissues (KW = 30.1, *p* < 0.0001). Muscle had significantly lower MMHg concentrations than hair (Dunnett: *p* = 0.006). All of the hooded seal tissues had significantly higher MMHg concentration than herring (Dunnett: *p* < 0.0001 for hair, muscle and kidney and *p* = 0.0003 for liver).

iHg concentrations in hooded seals followed the trend: liver ≈ kidney ≫ hair ≈ muscle (Table 1) with significant differences between tissue (KW = 32.3, *p* < 0.0001). Muscle and hair had significantly lower iHg concentrations than liver and kidney (Dunnett: <0.0001 for all). The liver and kidney of hooded seals had significantly higher iHg concentrations than herring (Dunnett: *p* < 0.0001 and *p* = 0.0001, respectively). Differences in iHg concentrations among the muscle and hair of hooded seals, and herring were weak (Dunnett: *p* > 0.01).

The percentage of MMHg in seals (fMMHg) followed the trend: hair ≈ muscle > liver ≈ kidney (Table 1), with significant differences between tissues (KW = 34.1, *p* < 0.0001). Hair had significantly higher fMMHg than liver and kidney (Dunnett: *p* = 0.006 and *p* = 0.0001, respectively). The liver and kidney of hooded seals had significantly lower fMMHg than herring (Dunnett: *p* < 0.0001 and *p* = 0.0002, respectively). The percentage of iHg in seals (fiHg) followed the trend: kidney ≈ liver > muscle ≈ hair (Table 1). Kidney and liver had significantly higher fiHg than muscle (KW = 27.5, *p* < 0.0001). Differences between kidney, liver, and hair were weak (Dunnett: *p* = 0.02 for both). The liver and kidney of hooded seals had significantly higher fiHg than herring (Dunnett: *p* = 0.0005 and *p* = 0.0007, respectively).

3.3. Mercury stable isotope composition

δ²⁰²Hg values significantly differed between hooded seal tissues (KW = 29.6, *p* < 0.0001), following the trend: hair > muscle > liver > kidney (Table 1). δ²⁰²Hg values were significantly different between the kidney of hooded seals and herring (*p* = 0.001) and hair and herring (*p* = 0.0004). No differences were found for Δ¹⁹⁹Hg, Δ²⁰¹Hg and Δ²⁰⁴Hg values. Δ²⁰⁰Hg values differed only between the muscle and kidney of hooded seals (*p* = 0.003), but this difference was within the analytical uncertainty determined by reference material replicate measurements (e.g., 0.16‰–0.21‰ for DOLT-5 and URM-254, respectively) and will not be interpreted. Δ¹⁹⁹Hg/Δ²⁰¹Hg slopes did not differ between tissues and ranged between 1.15 ± 0.05 in hooded seals liver to 1.20 ± 0.05 in herring muscle (Fig. 1, Table S5).

A positive correlation was found between δ²⁰²Hg values and fMMHg (Spearman ρ = 0.643, *p* = 0.0003, R² = 0.567). A negative correlation was found between δ²⁰²Hg values and fiHg (Spearman ρ = –0.705, *p* < 0.0001, R² = 0.587). A weak negative correlation was found between Δ¹⁹⁹Hg values and fiHg (Spearman ρ = –0.382, *p* = 0.048, R² = 0.106). No correlation was found between Δ¹⁹⁹Hg values and fMMHg (*p* = 0.051).

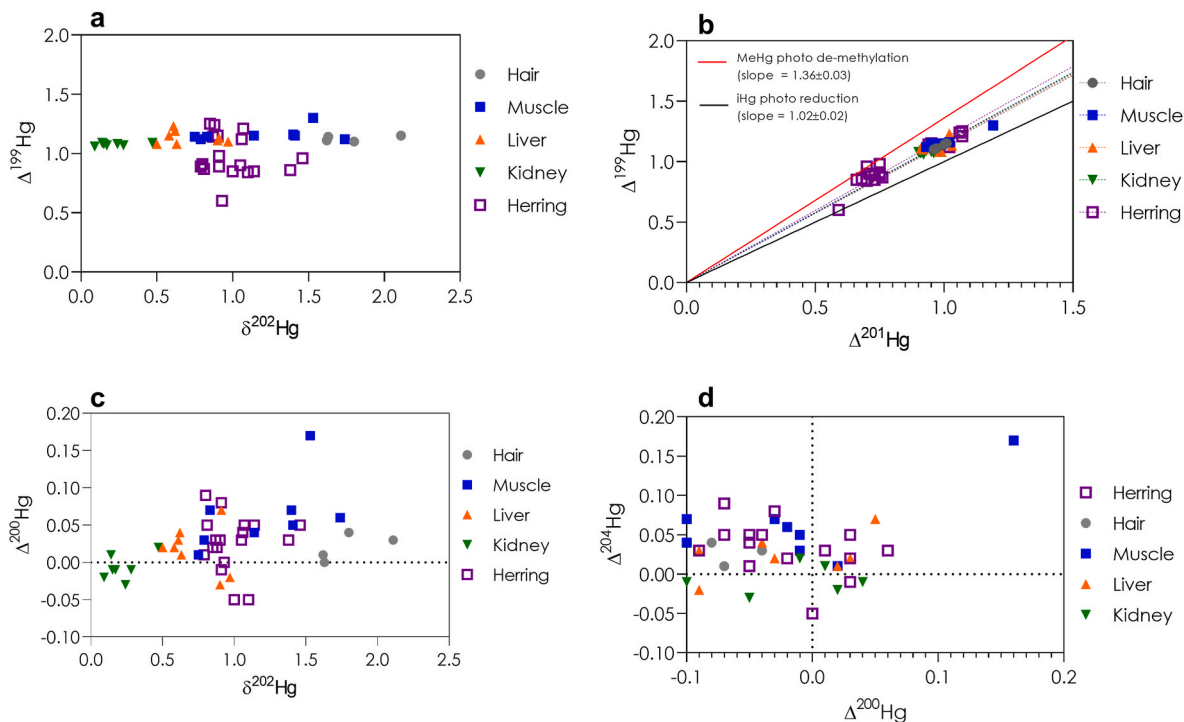


Fig. 1. Biplots of mercury stable isotope ratios: $\Delta^{199}\text{Hg}$ versus $\delta^{202}\text{Hg}$ (a), $\Delta^{199}\text{Hg}$ versus $\Delta^{201}\text{Hg}$ (b), $\Delta^{200}\text{Hg}$ versus $\delta^{202}\text{Hg}$ (c) and $\Delta^{204}\text{Hg}$ versus $\Delta^{200}\text{Hg}$ (d) in hair (grey square), muscle (blue square), liver (orange triangle), kidney (green down-triangle) of hooded seals *C. cristata* and their prey, the herring *C. Harengus* (purple open square). Data are shown in per mill ‰. (For interpretation of the references to colour in this figure legend, the reader is referred to the Web version of this article.)

3.4. Mercury trophic isotopic fractionation

In the following paragraphs, the difference in $\delta^{202}\text{Hg}$ values between the prey (herring) and the predator (hooded seal) resulting from Hg isotopic fractionation during dietary assimilation will be referred to as “trophic isotopic shift” or the “shift in $\delta(\text{or } \Delta)^x\text{Hg}$ values”. The shift in $\delta^{202}\text{Hg}$ values between hooded seals tissues and herring significantly differed between tissues (KW = 53.6, $p < 0.0001$), ranging from -0.28‰ between seals kidney and herring to 0.79‰ between seals hair and herring (Table S6). The shift in $\Delta^{199}\text{Hg}$ values between hooded seals and herring differed weekly ($p = 0.023$), ranging from 0.11‰ between seals kidney and herring to 0.19‰ between seals hair and herring. No differences were found between tissues for $\Delta^{201}\text{Hg}$ values between hooded seals and herring. $\Delta^{200}\text{Hg}$ variability was lower than the analytical uncertainty determined by reference material replicate measurements (e.g. 0.16‰ – 0.21‰ , for DOLT-5 and URM-254 respectively). As such they cannot be interpreted. No differences were found between tissues for $\Delta^{201}\text{Hg}$ and $\Delta^{204}\text{Hg}$ values between hooded seals tissues and herring.

4. Discussion

4.1. The influence of mercury trophic transfer on MDF and MIF signatures

Hg stable isotope odd-MIF is known to occur during photochemical processes in the environment (Tsui et al., 2019; Gehrke and Blum, 2011). Different odd-MIF values between tissues of Antarctic petrels have been attributed to the bioaccumulation of a mixture of MMHg sources rather than internal MIF (Renado et al., 2021). Thus, $\Delta^{199}\text{Hg}$ values should not differ between tissues when animals are exposed to Hg originating from a single environmental source (Pinzone et al., 2021b), not should they change from prey to predator (Tsui et al., 2019). Our data showed that $\Delta^{199}\text{Hg}$ values ranged between 0.97‰ (herring

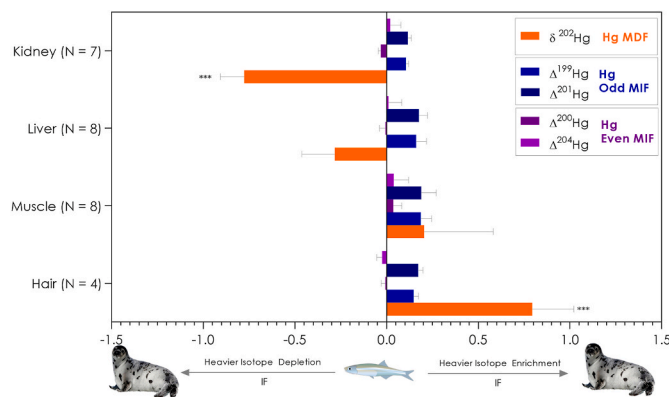


Fig. 2. Trophic Hg isotopic fractionation for Hg MDF ($\delta^{202}\text{Hg}$, in orange), Hg odd MIF ($\Delta^{199}\text{Hg}$ and $\Delta^{201}\text{Hg}$ in a blue palette) and Hg even MIF (represented by $\Delta^{200}\text{Hg}$ and $\Delta^{204}\text{Hg}$ in a purple palette). Hg trophic isotopic fractionation is calculated as the difference between Hg stable isotope values measured in tissues of hooded seals *C. cristata* in human care and the mean of those measured in muscle of their diet (the herring, *C. harengus*). Bars represent mean with SD. Three asterisks = $p < 0.0001$, indicating a significant difference in Hg isotopic composition between hooded seals and prey. The Kruskal-Wallis significance was set at $\alpha = 0.05$. Hg trophic isotopic fractionation values can be found in Supporting Information (Table S6). (For interpretation of the references to colour in this figure legend, the reader is referred to the Web version of this article.)

muscle) to 1.16‰ (seal liver and muscle), while $\Delta^{201}\text{Hg}$ values ranged between 0.81‰ (herring muscle) to 1.00‰ (seal muscle; Fig. 1). However, these values did not differ significantly (Table 1). The shift in the odd-MIF signatures from herring to seals ranged between 0.11‰ and 0.19‰ for $\Delta^{199}\text{Hg}$ values and between 0.12‰ and 0.19‰ for $\Delta^{201}\text{Hg}$ values (Fig. 2, Table S5). This prey-predator fractionation was within the

range of Hg odd-MIF analytical uncertainty (0.02–0.35‰, Table 1). These observations indicate that no odd-MIF occurs between the tissues of hooded seal subadults and their prey as a result of Hg metabolism. The subtle odd-MIF shown by our data may be linked to the selective transfer between prey and predator of MMHg and iHg pools from different environmental sources, which have different MIF signatures (Manceau et al., 2021). This hypothesis is supported by the large variability in herring odd-MIF values (e.g., $\Delta^{199}\text{Hg}$ SD: $\pm 0.35\text{‰}$, Table 1). This could also explain the absence of correlation between odd-MIF and fMMHg or fiHg in all of hooded seal tissues.

Even-MIF ($\Delta^{200}\text{Hg}$ and $\Delta^{204}\text{Hg}$) predominantly occurs in atmospheric samples (e.g., rain, snow) and is not believed to result from biological processes (Cai and Chen, 2015). As such, $\Delta^{200}\text{Hg}$ and $\Delta^{204}\text{Hg}$ values should not vary from one trophic level to the other (Blum and Baskaran, 2011). This was confirmed by our measurements, which showed no significant shift in $\Delta^{200}\text{Hg}$ and $\Delta^{204}\text{Hg}$ values from herring to hooded seals (Fig. 2 and Table S6). Overall, these findings confirm the absence of *in vivo* MIF in hooded seal tissues, confirming once again the potential use of odd- and even-MIF as tracers of marine MMHg and atmospheric Hg sources to Arctic top predators.

A significant positive shift was observed in $\delta^{202}\text{Hg}$ values from herring to hooded seal hair ($+0.79 \pm 0.23\text{‰}$), while a significant negative $\delta^{202}\text{Hg}$ shift was observed from herring to hooded seal kidney ($-0.78 \pm 0.13\text{‰}$, Fig. 2 and Table S6). These values were lower than previously reported MDFs between human hair and seafood ($\approx 2\text{‰}$) (Li et al., 2016) but similar to those reported between Baikal seals and their prey ($\approx 1\text{‰}$) (Perrot et al., 2010). The $\delta^{202}\text{Hg}$ trophic shift in hooded seal muscle ($+0.20 \pm 0.38\text{‰}$) was lower than that found in long-finned pilot whales ($\approx 0.55\text{‰}$). Past literature showed that significant MDF does not always occur between prey and predator (Kwon et al., 2012), but the reasons remain debatable. Previous studies focused on wild animals, where inter-individual and inter-specific differences in diet, life stages, or habitat distribution could influence the large variability of reported prey-predator MDF extents. In this study, the controlled feeding design eliminated biases linked with ecological and metabolic factors, isolating the prey-predator MDF shift caused solely by dietary assimilation. Our results showed that the range of $\delta^{202}\text{Hg}$ trophic shift between herring and hooded seal hair, muscle, liver and kidney was still quite large (0.09–2.11‰, Table 1), indicating that basal tissue-specific metabolism already leads to a large variability of prey-predator MDF extents. Therefore, significant MDF between prey and predator would be observed only when specific tissues of a predator.

4.2. iHg *in vivo* speciation influences the extents of Hg MDF in hooded seals' liver and kidney

In hooded seals in human care, the large variability in prey-predator $\delta^{202}\text{Hg}$ trophic shifts between tissues might reflect the diversity of Hg speciation processes. Hg speciation refers to the ensemble of *in vivo* reactions (e.g., demethylation or biomineralization) through which MMHg is transformed into inorganic Hg compounds after being absorbed in the body of a predator (Templeton and Fujishiro, 2017). For marine predators such as large fish, seabirds or marine mammals, diet represents the main pathway of exposure to Hg. After prey digestion, MMHg is absorbed through the intestine walls and transported by the blood stream towards other tissues (Ché et al., 2020). The primary targets of MMHg in the body are sulfhydryl (thiol; -SH) groups of low- and high-weight biological ligands (Ajsuvakova et al., 2020). MMHg complexation with these molecules appears to regulate the accumulation and elimination in the different organs (Wagemann et al., 1998; Bridges and Zalups, 2010). MMHg can either be accumulated by highly metabolic tissues like the liver, where it will be metabolized and stored mostly as inorganic Hg, or be directly transferred to inert tissues like hair, where it bioaccumulates over time in its organic form and is eventually excreted through molting.

A strong positive correlation was found between the bioaccumulated

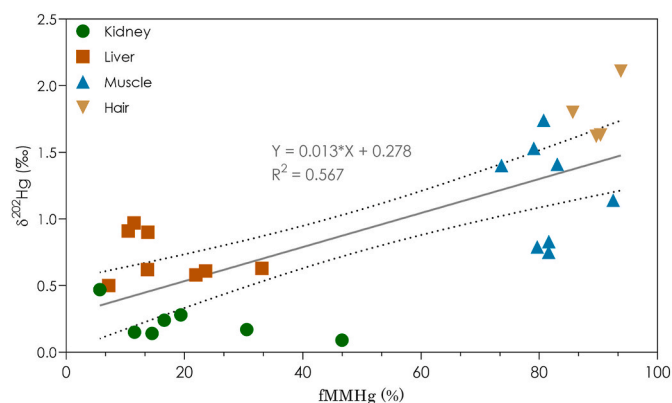


Fig. 3. Spearman's correlation between Hg MDF ($\delta^{202}\text{Hg}$, in ‰) and the fraction of MMHg over total Hg (fMMHg, in ‰) in hooded seal *C. cristata* in human care. Linear regression is represented by the straight grey line. Dotted lines show the 95 % confidential intervals. Kidney (green dot), Liver (dark-orange square), Muscle (turquoise triangle), Hair (gold down-triangle). (For interpretation of the references to colour in this figure legend, the reader is referred to the Web version of this article.)

fraction of MMHg (fMMHg) in each tissue and its $\delta^{202}\text{Hg}$ values (Fig. 3), in agreement with previous studies on long-finned pilot whales (Li et al., 2020). Hair and muscle presented the highest fMMHg (90 and 81%, respectively) and $\delta^{202}\text{Hg}$ values (1.79‰ and 1.20‰, respectively), while liver and kidney presented the lowest fMMHg (16‰ for both) and $\delta^{202}\text{Hg}$ values (0.71‰ and 0.22‰, respectively). These results suggest that in growing hooded seals *in vivo* Hg speciation processes, such as MMHg demethylation, significantly influence MDF the most; in accordance with Hg MDF findings in other true seal species and belugas (Perrot et al., 2015), long-finned pilot whales (Bolea-Fernandez et al., 2019; Li et al., 2020), Antarctic seabirds (Renedo et al., 2021) and European seabass (Pinzone et al., 2021b).

Liver is known to be the center of *in vivo* demethylation, where dietary MMHg is demethylated in Hg(II) and made inert, through coprecipitation of Hg(II) with selenium (Se) and formation of tienammite crystals (HgSe) (Kehrig et al., 2016). This process leads to the accumulation of Hg as iHg throughout the life of the individual. MMHg demethylation preferentially involves isotopically lighter MMHg, resulting in newly formed iHg characterized by lower $\delta^{202}\text{Hg}$ values (Pinzone et al., 2022). The remaining non-demethylated MMHg has higher $\delta^{202}\text{Hg}$ compared to the initially bioaccumulated MMHg⁵³. Because of the strong affinity for sulfhydryl groups of proteins, this isotopically heavier fraction of MMHg is preferentially redistributed towards tissues like muscle, brain and hair (Bridges and Zalups, 2010), which will ultimately exhibit higher $\delta^{202}\text{Hg}$ values and higher fMMHg over time (Fig. 3). This is observed in hooded seal hair and muscle, which are enriched in ^{202}Hg compared to liver.

In hooded seals in human care, kidney resulted as the isotopically lightest tissue (Table 1). This suggests that hepatic MMHg demethylation is not the only process affecting Hg MDF and $\delta^{202}\text{Hg}$ values. A review on Hg isotopy and internal dynamics published in 2020 highlighted the significant impact of biomineralization processes on ^{202}Hg fractionation in marine biota, depending on the profile of bioaccumulated Hg inorganic species (Li et al., 2022). Recent advances in laser-ablation or X-rays absorption techniques have provided more information on tissues-specific profiles of Hg species. Initially, it was believed that MMHg demethylation and HgSe bioaccumulation occurred solely in the liver. The first record of HgSe crystals in the Kupffer cells of Guiana dolphins suggested that these inorganic particles could reach the liver through the blood stream and accumulate locally, hypothesizing that MMHg detoxification processes occurred in multiple organs (Lailson-Brito et al., 2012). Using laser ablation ICP-MS on pilot whales tissues, Gajdosechova et al. (2016) demonstrated that after formation in the

liver, HgSe nanoparticles associate to selenium-rich structures and form larger iHg nodes that are found mostly in plasma (Gajdosechova et al., 2016). This was observed also in the brain (Gajdosechova et al., 2016). Subsequently, HgSe deposits of different size and weight were identified in muscle and liver of several species of other cetaceans (Ji et al., 2022), as well as liver, kidney, muscle and brain of bottlenose dolphins (von Hellfeld et al., 2024).

While liver has higher concentrations of Se-binding molecules, as demonstrated in several marine mammal species (e.g., Mediterranean Sea dolphins (Martínez-Ló et al., 2019)), the kidney is rich in thiol-containing molecules like metallothionines (MT) or glutathione (GSH) (Bridges and Zalups, 2017), making it the major endpoint of all iHg species (Zalups, 2000). This includes dietary iHg, isotopically lighter HgSe formed during MMHg breakdown in liver (Feng et al., 2015) or other tissues (Manceau et al., 2021; Rua-ibarz et al., 2019), and iHg species formed directly in the kidney from dietary MMHg⁷¹. Sonne et al. (2009) showed that concentrations of MTs were significantly higher in kidney of Greenland wild hooded seals compared to liver and that in kidney MT had higher Hg-binding capacity than Se (Sonne et al., 2009). These findings support the hypothesis that hooded seal kidney has a heterogenous profile of iHg species, while liver is dominated by HgSe crystals. A recent study on seabirds investigated the extent of Hg MDF during MMHg *in vivo* transformation processes using Hg compound specific stable isotope data and found that the largest hepatic fractionation of ²⁰²Hg occurs during MMHg (in the form of MMHg-Cys) biomineralization and transformation into inorganic HgSe precursors (e.g., Hg-tetraselenolate complex, Hg(Sec₄)), while no significant MDF occur during HgSe formation (Queipo-Abad et al., 2022). Although this analysis is not yet available for marine mammals, it supports the possibility that the bioaccumulation of different iHg species causes the lower $\delta^{202}\text{Hg}$ values observed in the kidney of hooded seals.

4.3. MMHg *in vivo* speciation influences the extents of Hg MDF in hooded seals' hair and muscle

Hair showed higher fMMHg than muscle (on average 90% and 81%, respectively) and higher $\delta^{202}\text{Hg}$ values (≥ 1 % of difference, Table 1). This shift could result from higher turnover rates in hair compared to muscle (Renedo et al., 2021). The term "turnover rate" refers to the duration required for a tissue to completely regenerate its cellular components, such as lipids, proteins, and carbohydrates (Mawson, 1955). Tissues with high turnover rates, such as muscles, livers, blood, and adipose tissue, are vital metabolic components. Continuous renewal of these tissues is essential for the proper functioning of the basal metabolism in animals (Vander Zanden et al., 2015). Inert tissues such as hair, nails, feathers, and bones have significantly longer turnover rates and may undergo renewal only once a year (Dauwe et al., 2003; Peterson et al., 2016). Although seal fur was found to be less efficient as an excretion route than feces, Grajewska et al. (2020) estimated that half of Hg excreted through grey seals' hair during molting was MMHg⁷⁸. In Antarctic seabirds, molting has been shown to promote the excretion of isotopically heavier MMHg, resulting in elevated Hg MDF and $\delta^{202}\text{Hg}$ values in feathers (Renedo et al., 2018). This process has also been demonstrated for human hair (Sherman et al., 2013; Laffont et al., 2011) and may be applicable to the hair of hooded seals. However hooded seal pups shed their lanugo in utero and present a distinctive "blueback" pelage after birth (Kovacs et al., 2018). This blue coat is maintained for about 2 years (Kovacs and Lavigne, 1986), after which the first molting occurs. The six pups analyzed in this study still had their blue coat at the time of euthanasia, suggesting that molting is an unlikely factor contributing to increased $\delta^{202}\text{Hg}$ values in their hair.

An alternative explanation for the observed trend may be attributed to redistribution dynamics of the different MMHg pools. In a previous publication, we proposed that the higher $\delta^{34}\text{S}$ values found in the hair of the same hooded seal pups in human care, compared to muscle were related to a preferential uptake of the dietary S pool by keratinized

tissues (Pinzone et al., 2017). Similarly, our data on hooded seals' liver and kidney suggested that the inter-tissue speciation of iHg pools is a crucial driver of Hg isotopic fractionation. The same could be proposed for hair and muscle, where, based on the tissue content in Hg thiol-ligands, the different species (and or pools) of MMHg could be more efficiently transferred to one tissue compared to another. While seal fur or birds feathers are the major direct endpoints of dietary MMHg, there is growing evidence of several MMHg and iHg species accumulating in muscle tissue (Ché et al., 2020). Therefore, in these hooded seals, the higher $\delta^{202}\text{Hg}$ values in hair could be linked with a more homogenous Hg pool coming from liver demethylation and biomineralization processes, while muscle could show a mix of Hg pools from the liver as well as directly from the diet.

4.4. Age influences Hg metabolism and mass-dependent fractionation in tissues of marine mammals

Previously, we proposed that age is a crucial factor influencing isotopic fractionation of C, N and S in seals (Pinzone et al., 2017). This could also apply to *in vivo* Hg MDF. When compared to the literature (Table 2), the liver and kidney of hooded seals in human care exhibited higher and positive $\delta^{202}\text{Hg}$ values than Baikal seals (Perrot et al., 2015), long-finned pilot whales (Bolea-Fernandez et al., 2019) and ringed seals from Alaska (Masbou et al., 2015). This may be linked to the fact that the hooded seals sampled in this study were all two-year-old growing subadults. Demethylation of MMHg in liver and Hg complexation with thiol-ligands in kidney are two detoxification mechanisms that develop with age as a consequence of the increasing exposure to this pollutant (Dietz et al., 2013). Studies have reported that young marine mammals do not reach the specific threshold of hepatic and renal MMHg concentrations that adults do (Bolea-Fernandez et al., 2019; Ewald et al., 2019). At a young age, the kidney appears to be as important as liver in stocking dietary Hg (mostly in the form of iHg), as MMHg *in vivo* breakdown is not very efficient. Over time, with the development of hepatic cellular composition, a greater proportion of iHg would be produced and redistributed from liver to the kidney (Ewald et al., 2019). We can hypothesize that this could change the isotopic composition of the remobilized iHg. Because isotopically lighter MMHg is preferentially selected for demethylation, this initially results in the production of a pool of very isotopically light iHg, which is then redistributed to the kidney. With the increased efficiency in Hg detoxification in older individuals, the rates of hepatic MMHg demethylation would also increase. As all the lighter MMHg is demethylated, the heavier Hg pool will be used, producing iHg enriched in ²⁰²Hg.

At the same time, hepatic molar Se:THg ratios were found to decrease with age in both pinnipeds and other cetaceans, signaling a change in the expression and availability of selenoproteins (e.g., selenoneine) between mature individuals and subadults (Houde et al., 2020). Li et al. (2020) proposed that the limitation of Se-binding proteins in older pilot whales could inhibit sequestration in liver of labile iHg as HgSe and lead to the circulation of ²⁰²Hg-depleted iHg out of the liver to other organs such as kidney. This might explain the lower $\delta^{202}\text{Hg}$ values in adult marine mammals in comparison to the hooded seal pups in human care. Nowadays, captivity of marine mammals for research purposes is strongly restricted, especially concerning adult individuals. Additionally, the hooded seal is included into the IUCN Red List as "vulnerable" (Kovacs and seal, 2016) and has been considered as "critically endangered" both at national (Kålå et al., 2010) and international level (ICES, 2019). For these reasons, it was not possible to include a control group of adult hooded seals in the feeding experiment. Therefore, our interpretation remains hypothetical.

Even if these hypotheses explain the difference in Hg MDF between hooded seals subadults and adult marine mammals, they do not justify the difference between $\delta^{202}\text{Hg}$ values measured in the liver and kidney of hooded seal pups and those reported for young individuals pilot whales (Table 2). Part of Hg MDF that cannot be explained by metabolic

Table 2

Literature review of known THg ($\mu\text{g g}^{-1}$ dw), MMHg fractions (as %) and Hg stable isotope ratios (in ‰) in marine mammals. Data are shown as Mean \pm SD when possible; otherwise as Min – Max or single measured value. Age groups are shown as: Juv = juveniles, Adu = adults, all = when age is not provided. Numbers in brackets represent the n = number of replicates. na = not available.

Study	Species	Tissue	Age	THg	%MMHg	$\delta^{202}\text{Hg}$	$\Delta^{199}\text{Hg}$	$\Delta^{201}\text{Hg}$	$\Delta^{199}\text{Hg}/\Delta^{201}\text{Hg}$	
Masbou et al., 2015	Ringed seal	Liver	Juv (3)	0.2 \pm 0.2	20 \pm 12	0.11 \pm 0.37	0.68 \pm 0.26	0.54 \pm 0.24	1.3 \pm 0.17	
			Adu (5)	2.9 \pm 1.8	9 \pm 9	-0.26 \pm 0.13	0.52 \pm 0.07	0.42 \pm 0.07	1.25 \pm 0.07	
Perrot et al., 2015	Ringed seal	Liver	all (4)	2.5 \pm 4.2	32 \pm 16	0.63 \pm 0.77	4.61 \pm 0.75	3.61 \pm 0.57	1.28 \pm 0.02	
			Muscle	all (6)	0.3 \pm 0.3	82 \pm 2	1.88 \pm 0.20	3.50 \pm 1.87	3.93 \pm 0.14	1.27 \pm 0.01
Masbou et al., 2018	Beluga	Liver	Adu (11)	40 \pm 41	10 \pm 7	-1.27 \pm 0.20	-0.06 \pm 0.07	-0.14 \pm 0.08	0.92 \pm 0.25	
	Baikal seal	Liver	Juv (2)	0.8–6.5	19–42	-0.43 - 1.1	4.66–4.91	3.66–3.86	1.27 \pm 0.01	
			Adu (1)	19	6	-0.65	3.21	2.52	1.27	
	Kidney	Juv (1)	2.8	24	-0.49	4.47	3.53	1.27		
		Adu (1)	8.0	8	-0.64	3.64	2.88	1.26		
		Muscle	Adu (1)	0.7	87	2.35	4.02	3.13	1.28	
		Hair	Adu (1)	2.5	81	2.39	5.13	4.23	1.21	
	Beluga	Liver	nd (4)	21 \pm 24	9 \pm 6	-0.28 \pm 1.06	0.03 \pm 0.21	-0.03 \pm 0.17	0.91 \pm 0.46	
			Adu (15)	41 \pm 33	15 \pm 19	-1.18 \pm 0.20	-0.06 \pm 0.08	-0.15 \pm 0.08	0.84 \pm 2.37	
	Polar bear	Liver	Juv (1)	5.6	na	-0.07	0.53	0.35	1.51	
			nd (7)	18 \pm 18	na	0.05 \pm 0.27	0.50 \pm 0.18	0.37 \pm 0.18	1.30 \pm 0.08	
			Adu (7)	10 \pm 4.1	na	0.33 \pm 0.35	0.61 \pm 0.29	0.48 \pm 0.26	1.37 \pm 0.24	
Bolea-Fernandez et al., 2019	Pilot whale	Liver	Juv (10)	11 \pm 14	19 \pm 9	-0.84 \pm 0.30	1.04 \pm 0.06	0.87 \pm 0.04	1.19 \pm 0.06	
			Adu (11)	255 \pm 174	2 \pm 1	-0.60 \pm 0.25	1.03 \pm 0.05	0.84 \pm 0.05	0.84 \pm 0.05	
	Kidney	Juv (10)	1.5 \pm 0.9	34 \pm 8	-0.59 \pm 0.23	1.05 \pm 0.05	0.86 \pm 0.04	0.86 \pm 0.04		
		Adu (11)	11 \pm 6.4	14 \pm 8	-0.74 \pm 0.16	1.03 \pm 0.05	0.85 \pm 0.06	1.21 \pm 0.09		
	Muscle	Juv (9)	1.1 \pm 0.5	90 \pm 7	0.72 \pm 0.22	1.07 \pm 0.05	0.90 \pm 0.03	0.90 \pm 0.06		
		Adu (6)	4.0 \pm 0.5	83 \pm 14	0.39 \pm 0.15	1.07 \pm 0.06	0.90 \pm 0.03	1.19 \pm 0.05		
	Blood	Juv (7)	na	na	1.06 \pm 0.10	1.09 \pm 0.04	0.91 \pm 0.03	0.91 \pm 0.03		
		Adu (7)	na	na	1.06 \pm 0.13	1.11 \pm 0.05	0.93 \pm 0.05	1.20 \pm 0.07		
	Li et al., 2020	Pilot whale	Kidney	Juv (3)	13 \pm 7.5	21 \pm 6	-0.87 \pm 0.17	1.05 \pm 0.06	0.88 \pm 0.03	1.19 \pm 0.08
				Adu (4)	41 \pm 14	12 \pm 4	-0.74 \pm 0.09	1.00 \pm 0.06	0.86 \pm 0.04	1.15 \pm 0.05
Liver		Juv (3)	69 \pm 62	17 \pm 5	-0.70 \pm 0.27	0.96 \pm 0.09	0.84 \pm 0.05	1.13 \pm 0.10		
		Adu (4)	509 \pm 253	5 \pm 2	-0.16 \pm 0.37	0.86 \pm 0.07	0.83 \pm 0.09	1.12 \pm 0.16		
Pinzone PhD 2021	Hooded seal	Muscle	Juv (7)	0.5 \pm 0.2	90 \pm 2	0.79 \pm 0.26	0.90 \pm 0.12	0.74 \pm 0.10	1.21 \pm 0.05	
			Adu (12)	1.8 \pm 1.6	91 \pm 2	1.09 \pm 0.36	0.82 \pm 0.22	0.69 \pm 0.19	1.21 \pm 0.09	
	Ringed seal	Muscle	Juv (7)	1.8 \pm 1.0	84 \pm 6	0.04 \pm 0.34	0.79 \pm 0.14	0.61 \pm 0.11	1.30 \pm 0.08	
			Adu (9)	1.1 \pm 0.4	83 \pm 6	0.22 \pm 0.20	0.68 \pm 0.18	0.54 \pm 0.14	1.26 \pm 0.06	
	Harp seal	Muscle	Juv (3)	0.7 \pm 0.2	89 \pm 1	1.01 \pm 0.25	0.67 \pm 0.11	0.54 \pm 0.09	1.25 \pm 0.06	
			Adu (6)	0.6 \pm 0.4	91 \pm 0.1	1.15 \pm 0.29	0.77 \pm 0.14	0.63 \pm 0.15	1.23 \pm 0.06	
This study	Hooded seal	Liver	Juv (6)	7.8 \pm 3.5	17 \pm 9	0.71 \pm 0.36	1.16 \pm 0.13	0.99 \pm 0.009	1.15 \pm 0.05	
			Kidney	Juv (6)	5.4 \pm 2.6	16 \pm 8	0.22 \pm 0.26	1.08 \pm 0.02	0.93 \pm 0.04	1.16 \pm 0.03
		Muscle	Juv (6)	0.5 \pm 0.1	81 \pm 5	1.20 \pm 0.76	1.16 \pm 0.12	1.00 \pm 0.16	1.16 \pm 0.04	
			Hair	Juv (4)	1.2 \pm 0.3	90 \pm 3	1.79 \pm 0.45	1.12 \pm 0.05	0.99 \pm 0.05	1.14 \pm 0.003

activity may relate to the difference in foraging habitat and diet. Our study is the first assessing Hg isotopic composition in animals in human care on a constant diet, while all the other studies use samples of wild animals. Unlike this study, Hg stable isotope ratios reported in these works might be influenced by shifts in diet, distribution and behavior. Future research efforts are needed to evaluate the mechanisms and isotopic fractionation of the different species of Hg bioaccumulated by marine mammals in different tissues, across sex and age groups.

5. Conclusions

Our main goal was to investigate the Hg trophic isotopic fractionation dynamics resulting from tissue-specific basal metabolism of hooded seals, independent of diet, distribution, and age. Our initial findings confirmed that Hg odd and even MIF values ($\Delta^{199}\text{Hg}$, $\Delta^{201}\text{Hg}$, and $\Delta^{200}\text{Hg}$, $\Delta^{204}\text{Hg}$) remain consistent from prey to consumer, establishing their utility as tracers of Hg sources in Arctic seals. Additionally, we demonstrated that Hg speciation (organic versus inorganic pools) linked to tissue-specific metabolism influences MDF ($\delta^{202}\text{Hg}$). This also emphasizes the importance of selecting an appropriate tissue for Hg isotope analysis based on the study's specific objectives. Our results also support what was proposed in other seal and cetacean species about the influence of age on Hg internal isotopic incorporation in Arctic true seals. This must be considered when comparing Hg trophic enrichment

and stable isotope ratios across studies. Our study presents a new perspective on the interpretation of Hg stable isotopes in highly specialized top predators such as Arctic seals. Future studies can build on these findings to gain a deeper understanding of Hg cycling and accumulation in Arctic ecosystems.

CRedit authorship contribution statement

Marianna Pinzone: Writing – original draft, Visualization, Project administration, Methodology, Investigation, Data curation, Conceptualization. **David Amouroux:** Validation, Data curation, Conceptualization. **Emmanuel Tessier:** Writing – review & editing, Methodology, Investigation. **Mario Acquarone:** Writing – review & editing, Resources. **Ursula Siebert:** Writing – review & editing, Resources. **Krishna Das:** Writing – review & editing, Validation, Supervision, Funding acquisition, Conceptualization.

Declaration of competing interest

The authors declare that they have no known competing financial interests or personal relationships that could have appeared to influence the work reported in this paper.

Data availability

The raw data are presented in the Supporting Information

Acknowledgments

The authors would like to thank prof. Lars Folkow and his team at the UiT – The Arctic University of Norway in Tromsø – for giving us access to the samples of captive seals and herring. The authors thank the members of the IPREM institute from Pau University for their warm welcome and for sharing their knowledge and expertise with us. Special thanks to Sylvaine Bérail and Tiago Caetano for their practical assistance in samples preparation and GC-ICP-MS analysis. Marianna Pinzone was supported by a FRIA doctoral fellowship (Fund for Research Training in Industry and in Agriculture). KD is a Senior FRS-FNRS Research Associate. The analyses were also funded through a F.R.S.-FNRS Research Credit scholarship (IsoArctic project, J.0030.19).

Appendix A. Supplementary data

Supplementary data to this article can be found online at <https://doi.org/10.1016/j.envpol.2024.124450>.

References

- Ajsuvakova, O.P., et al., 2020. Sulfhydryl groups as targets of mercury toxicity the binding of Hg to Cys mediates multiple toxic effects. *Coord. Chem. Rev.* 417.
- Alvira-Iraizoz, F., Nordøy, E.S., 2019. Evidence of seawater drinking in fasting subadult hooded seals (*Cystophora cristata*). *J. Anim. Behav. Biometeorol.* 7, 52–59.
- Bérail, S., et al., 2017. Determination of total Hg isotopic composition at ultra-trace levels by on line cold vapor generation and dual gold-amalgamation coupled to MC-ICP-MS. *J. Anal. At. Spectrom.* 32, 373–384.
- Blix, A.S., 2005. Arctic Animals and Their Adaptations of Life on the Edge. Tapir Academic Press.
- Blix, A.S., 2016. Adaptations to polar life in mammals and birds. *J. Exp. Biol.* 219, 1093–1105.
- Blum, J.D., 2011. Applications of stable mercury isotopes to biogeochemistry. In: Baskaran, M. (Ed.), *Handbook of Environmental Isotope Geochemistry*. Springer, pp. 229–245.
- Bolea-Fernandez, E., Rua-Ibarz, A., Krupp, E.M., Feldmann, J., Vanhaecke, F., 2019. High-precision isotopic analysis sheds new light on mercury metabolism in long-finned pilot whales (*Globicephala melas*). *Sci. Rep.* 9, 7262.
- Bowen, W.D., Oftedal, O.T., Boness, D.J., 1985. Birth to weaning in 4 days: remarkable growth in the hooded seal, *Cystophora cristata*. *Can. J. Zool.* 63, 2841–2846.
- Bridges, C.C., Zalups, R.K., 2010. Transport of inorganic mercury and methylmercury in target tissues and organs. *J. Environ. Heal. B Crit. Rev.* 13, 385–410.
- Bridges, C.C., Zalups, R.K., 2017. Mechanisms involved in the transport of mercuric ions in target tissues. *Arch. Toxicol.* 91, 63–81.
- Brunborg, L.A., Graff, I.E., Frøyland, L., Julshamn, K., 2006. Levels of non-essential elements in muscle from harp seal (*Phagophilus groenlandicus*) and hooded seal (*Cystophora cristata*) caught in the Greenland Sea area. *Sci. Total Environ.* 366, 784–798.
- Cai, H., Chen, J., 2015. Mass-independent Fractionation of Even Mercury Isotopes. <https://doi.org/10.1007/s11434-015-0968-8>.
- Caut, S., Angulo, E., Courchamp, F., 2009. Variation in discrimination factors ($\Delta^{15}N$ and $\Delta^{13}C$): the effect of diet isotopic values and applications for diet reconstruction. *J. Appl. Ecol.* 46, 443–453.
- Chételat, J., Ackerman, J.T., Eagles-Smith, C.A., Hebert, C.E., 2020. Methylmercury exposure in wildlife: a review of the ecological and physiological processes affecting contaminant concentrations and their interpretation. *Sci. Total Environ.* 711, 135117.
- Clémens, S., Monperrus, M., Donard, O.F.X., Amouroux, D., Guérin, T., 2012. Mercury speciation in seafood using isotope dilution analysis: a review. *Talanta* 89, 12–20.
- Cransveld, A., et al., 2017. Mercury stable isotopes discriminate different populations of European seabass and trace potential Hg sources around Europe. *Environ. Sci. Technol.* 51, 12219–12228.
- Dauwe, T., Bervoets, L., Pinxten, R., Blust, R., Eens, M., 2003. Variation of heavy metals within and among feathers of birds of prey: effects of molt and external contamination. *Environ. Pollut.* 124, 429–436.
- Dietz, R., et al., 2013. What are the toxicological effects of mercury in Arctic biota. *Sci. Total Environ.* 443, 775–790.
- Dietz, R., et al., 2019. Current state of knowledge on biological effects from contaminants on arctic wildlife and fish. *Sci. Total Environ.* 696, 133792.
- Eagles-Smith, C.A., et al., 2018. Modulators of mercury risk to wildlife and humans in the context of rapid global change. *Ambio* 47, 170–197.
- Epov, V.N., et al., 2008. Simultaneous determination of species-specific isotopic composition of Hg by gas chromatography coupled to multicollector ICPMS. *Anal. Chem.* 80, 3530–3538.
- Ewald, J.D., Kirk, J.L., Li, M., Sunderland, E.M., 2019. Organ-specific differences in mercury speciation and accumulation across ringed seal (*Phoca hispida*) life stages. *Sci. Total Environ.* 650, 2013–2020.
- Feng, C., et al., 2015. Specific pathways of dietary methylmercury and inorganic mercury determined by mercury speciation and isotopic composition in zebrafish (*Danio rerio*). *Environ. Sci. Technol.* 49, 12984–12993.
- Gajdosechova, Z., et al., 2016. In vivo formation of natural HgSe nanoparticles in the liver and brain of pilot whales. *Sci. Rep.* 6, 1–11.
- Gehrke, G.E., Blum, J.D., 2011. Mercury Cycling in the Marine Environment: Insights from Mercury Stable Isotopes. University of Michigan.
- Geiseler, S.J., Larson, J., Folkow, L.P., 2016. Synaptic transmission despite severe hypoxia in hippocampal slices of the deep-diving hooded seal. *Neuroscience* 334, 39–46.
- Gentry, R.L., Holt, J.R., 1982. Equipment and techniques for handling northern fur seals. NOAA Tech. Rep. 15. NMFS SSRF-758.
- Germain, L.R., Koch, P.L., Harvey, J., McCarthy, M.D., 2013. Nitrogen isotope fractionation in amino acids from harbor seals: implications for compound-specific trophic position calculations. *Mar. Ecol. Prog. Ser.* 482, 265–277.
- Grajewska, A., Falkowska, L., Saniewska, D., Pawliczka, I., 2020. Fur and faeces – routes of mercury elimination in the Baltic grey seal (*Halichoerus grypus grypus*). *Sci. Total Environ.* 717, 137050.
- Hoff, M.L.M., Fabrizius, A., Czech-Damal, N.U., Folkow, L.P., Burmester, T., 2017. Transcriptome analysis identifies key metabolic changes in the hooded seal (*Cystophora cristata*) brain in response to hypoxia and reoxygenation. *PLoS One* 12, 1–21.
- Houde, M., et al., 2020. Mercury in ringed seals (*Phoca hispida*) from the Canadian arctic in relation to time and climate parameters. *Environ. Toxicol. Chem.* 00, 1–13.
- ICES, 2019. Ices/nafo/nammco working group on harp and hooded seals (WGHARP). ICES Sci. reports 1, 193pp.
- Ji, X., et al., 2022. Identification of mercury-containing nanoparticles in the liver and muscle of cetaceans. *J. Hazard Mater.* 424, 127759.
- Julshamn, K., Grahl-Nielsen, O., 2000. Trace element levels in harp seal (*Phagophilus groenlandicus*) and hooded seal (*Cystophora cristata*) from the Greenland Sea. A multivariate approach. *Sci. Total Environ.* 250, 123–133.
- Kålås, J.A., Viken, Å., Henriksen, S., Skjelseth, S., 2010. Norsk rødliste for arter. https://artsdatabanken.no/taxon/_/48048 (2010).
- Katz, S.A., Chatt, A., 1988. Hair Analysis : Applications in the Biomedical and Environmental Sciences. VCH Publishers, New York. Weinheim : VCH Verlagsgesellschaft.
- Kehrig, H.A., Hauser-Davis, R.A., Seixas, T.G., Pinheiro, A.B., Di Benedetto, A.P.M., 2016. Mercury species, selenium, metallothioneins and glutathione in two dolphins from the southeastern Brazilian coast: mercury detoxification and physiological differences in diving capacity. *Environ. Pollut.* 213, 785–792.
- Kovacs, K.M., Lavigne, D.M., 1986. Maternal investment and neonatal growth in phocid seals. *J. Anim. Ecol.* 55, 1035–1051.
- Kovacs, K.M., 2018. Hooded seal, *Cystophora cristata*. In: Wursig, B., Thewissen, J.G.M., Kovacs, K.M. (Eds.), *Encyclopedia of Marine Mammals*, pp. 477–478.
- Kovacs, K.M. *Cystophora cristata*, seal, Hooded, 2016. IUCN Red List Threat. Species 2016 e.T6204A45225150. T6204A45225150.
- Kwon, S.Y., et al., 2012. Absence of fractionation of mercury isotopes during trophic transfer of methylmercury to freshwater fish in captivity. *Environ. Sci. Technol.* 46, 7527–7534.
- Kwon, S.Y., Blum, J.D., Chen, C.Y., Meatey, D.E., Mason, R.P., 2014. Mercury isotope study of sources and exposure pathways of methylmercury in estuarine food webs in the northeastern U.S. *Environ. Sci. Technol.* 48, 10089–10097.
- Kwon, S.Y., et al., 2020. Mercury stable isotopes for monitoring the effectiveness of the Minamata Convention on Mercury. *Earth-Science Rev.* 203, 103111.
- Laffont, L., et al., 2011. Hg speciation and stable isotope signatures in human hair as a tracer for dietary and occupational exposure to mercury. *Environ. Sci. Technol.* 45, 9910–9916.
- Lailson-Brito, J., et al., 2012. Mercury-selenium relationships in liver of Guiana dolphin: the possible role of kupffer cells in the detoxification process by tiemannite formation. *PLoS One* 7, e42162.
- Le Croizier, G., et al., 2020. Mercury isotopes as tracers of ecology and metabolism in two sympatric shark species. *Environ. Pollut.* 265.
- Lehnherr, I., 2014. Methylmercury biogeochemistry: a review with special reference to Arctic aquatic ecosystems. *Environ. Rev.* 22, 229–243.
- Li, M., et al., 2014. Assessing sources of human methylmercury exposure using stable mercury isotopes. *Environ. Sci. Technol.* 48, 8800–8806.
- Li, M., et al., 2016. Insights from mercury stable isotopes into factors affecting the internal body burden of Methylmercury in frequent fish consumers. *Elementa* 2016, 1–13.
- Li, M., et al., 2020. Selenium and stable mercury isotopes provide new insights into mercury toxicokinetics in pilot whales. *Sci. Total Environ.* 710, 136325.
- Li, M.L., et al., 2022. Internal dynamics and metabolism of mercury in biota: a review of insights from mercury stable isotopes. *Environ. Sci. Technol.* 56, 9182–9195.
- Man, Y., et al., 2019. Primary amino acids affect the distribution of methylmercury rather than inorganic mercury among tissues of two farmed-raised fish species. *Chemosphere* 225, 320–328.
- Manceau, A., et al., 2021. Mercury isotope fractionation by internal demethylation and biomineralization reactions in seabirds: implications for environmental mercury science. *Environ. Sci. Technol.* 55, 13942–13952.
- Martínez-López, E., Peñalver, J., Lara, L., García-Fernández, A.J., 2019. Hg and Se in organs of three cetacean species from the murcia coastline (Mediterranean Sea). *Bull. Environ. Contam. Toxicol.* 103, 521–527.

- Masbou, J., Point, D., Sonke, J.E., 2013. Application of a selective extraction method for methylmercury compound specific stable isotope analysis (MeHg-CSIA) in biological materials. *J. Anal. At. Spectrom.* 28, 1620–1628.
- Masbou, J., et al., 2015. Hg stable isotope time trend in ringed seals registers decreasing Sea ice cover in the alaskan arctic. *Environ. Sci. Technol.* 49, 8977–8985.
- Mawson, C.A., 1955. Meaning of 'turnover' in biochemistry. *Nature* 176, 317.
- Meng, M., et al., 2020. Mercury isotope variations within the marine food web of Chinese Bohai Sea: implications for mercury sources and biogeochemical cycling. *J. Hazard Mater.* 384, 121379.
- Nielsen, C.O., Dietz, R., 1990. Distributional pattern of zinc, cadmium, mercury, and selenium in livers of Hooded Seal (*Cystophora cristata*). *Biol. Trace Elem. Res.* 24, 61–71.
- Øigård, T.A., Haug, T., Nilssen, K.T., 2014. Current status of hooded seals in the Greenland Sea. Victims of climate change and predation? *Biol. Conserv.* 172, 29–36.
- Perrot, V., et al., 2010. Tracing sources and bioaccumulation of mercury in fish of lake Baikal— angara river using Hg isotopic composition. *Environ. Sci. Technol.* 44, 8030–8037.
- Perrot, V., et al., 2015. Natural Hg isotopic composition of different Hg compounds in mammal tissues as a proxy for in vivo breakdown of toxic methylmercury. *Metallomics* 8, 170–178.
- Peterson, S.H., Ackerman, J.T., Costa, D.P., 2016. Mercury correlations among blood, muscle, and hair of northern elephant seals during the breeding and molting fasts. *Environ. Toxicol. Chem.* 35, 2103–2110.
- Pinzone, M., et al., 2017. Carbon, nitrogen and sulphur isotopic fractionation in captive juvenile hooded seal (*Cystophora cristata*): application for diet analysis. *Rapid Commun. Mass Spectrom.* 31, 1720–1728.
- Pinzone, M., et al., 2021a. First record of plastic debris in the stomach of a hooded seal pup from the Greenland Sea. *Mar. Pollut. Bull.* 167, 112350.
- Pinzone, M., et al., 2021b. Contamination levels and habitat use influence Hg stable isotopes and accumulation in the European seabass *Dicentrarchus labrax*. *Environ. Pollut.* 281.
- Pinzone, M., et al., 2022. Dynamics of dietary mercury determined by mercury speciation and isotopic composition in *Dicentrarchus labrax*. *Front. Environ. Chem.* 3, 1–13.
- Poulin, B.A., et al., 2021. Isotope fractionation from in vivo methylmercury detoxification in waterbirds. *ACS Earth Sp. Chem.* 5, 990–997.
- Queipo-Abad, S., et al., 2022. New insights into the biomineralization of mercury selenide nanoparticles through stable isotope analysis in giant petrel tissues. *J. Hazard Mater.* 425, 127922.
- Renedo, M., et al., 2017. Assessment of Mercury Speciation in Feathers Using Species-specific Isotope Dilution Analysis. <https://doi.org/10.1016/j.talanta.2017.05.081>.
- Renedo, M., Amouroux, D., Pedrero, Z., Bustamante, P., Cherel, Y., 2018. Identification of sources and bioaccumulation pathways of MeHg in subantarctic penguins: a stable isotopic investigation. *Sci. Rep.* 8, 1–11.
- Renedo, M., Pedrero, Z., Amouroux, D., Cherel, Y., Bustamante, P., 2021. Mercury isotopes of key tissues document mercury metabolic processes in seabirds. *Chemosphere* 263, 127777.
- Rodríguez-González, P., Manuel Marchante-Gayón, J., Ignacio García Alonso, J.T., Sanz-Medel, A., 2005. Isotope dilution analysis for elemental speciation: a tutorial review. *Spectrochim. Acta, Part B* 60, 151–207.
- Routti, H., Jenssen, B.M., Tartu, S., 2018. Ecotoxicologic stress in Arctic marine mammals, with particular focus on polar bears. *Marine Mammal Ecotoxicology: Impacts of Multiple Stressors on Population Health*. Elsevier Inc. <https://doi.org/10.1016/B978-0-12-812144-3.00013-9>
- Rua-ibarz, A., et al., 2019. Characterization of Natural and Affected Environments Tracing Mercury Pollution along the Norwegian Coast via Elemental, Speciation and Isotopic Analysis of Liver and Muscle Tissue of Deep-Water Marine Fish (*Brosme Brosme*). <https://doi.org/10.1021/acs.est.8b04706>.
- Sherman, L.S., Blum, J.D., Franzblau, A., Basu, N., 2013. New insight into biomarkers of human mercury exposure using naturally occurring mercury stable isotopes. *Environ. Sci. Technol.* 47, 3403–3409.
- Sonne, C., et al., 2009. A study of metal concentrations and metallothionein binding capacity in liver, kidney and brain tissues of three Arctic seal species. *Sci. Total Environ.* 407, 6166–6172.
- Templeton, D.M., Fujishiro, H., 2017. Terminology of elemental speciation – an IUPAC perspective. *Coord. Chem. Rev.* 352, 424–431.
- Tsui, M.T.K., Blum, J.D., Kwon, S.Y., 2019. Review of stable mercury isotopes in ecology and biogeochemistry. *Sci. Total Environ.* 135386 <https://doi.org/10.1016/j.scitotenv.2019.135386>.
- Vander Zanden, M.J., Clayton, M.K., Moody, E.K., Solomon, C.T., Weidel, B.C., 2015. Stable isotope turnover and half-life in animal tissues: a literature synthesis. *PLoS One* 10, 1–16.
- von Hellfeld, R., et al., 2024. High resolution visualisation of tiemannite microparticles, essential in the detoxification process of mercury in marine mammals. *Environ. Pollut.* 342, 123027.
- Wagemann, R., Trebacz, E., Boila, G., Lockhart, W.L., 1998. Methylmercury and total mercury in tissues of arctic marine mammals. *Sci. Total Environ.* 218, 19–31.
- Wang, W.X., Tan, Q.G., 2019. Applications of dynamic models in predicting the bioaccumulation, transport and toxicity of trace metals in aquatic organisms. *Environ. Pollut.* 252, 1561–1573.
- Yamakawa, A., Takeuchi, A., Shibata, Y., Berail, S., Donard, O.F.X., 2016. Determination of Hg isotopic compositions in certified reference material NIES No. 13 Human Hair by cold vapor generation multi-collector inductively coupled plasma mass spectrometry. *Accredit. Qual. Assur.* 21, 197–202.
- Zalups, R.K., 2000. Molecular interactions with mercury in the kidney. *Pharmacol. Rev.* 52, 113–143.
- Zhou, Z., Wang, H., Li, Y., 2023. Mercury stable isotopes in the ocean: analytical methods, cycling, and application as tracers. *Sci. Total Environ.* 874, 162485.